SUPPLEMENTARY MATERIAL FOR DEPOSITION

DETERMINATION OF THE NUCLEATION MECHANISM AND KINETICS FROM THE ANALYSIS OF POLYTHERMAL CRYSTALLISATION DATA: METHYL STEARATE FROM KEROSENE SOLUTIONS

Diana M. Camacho Corzo[a], Antonia Borissova[a], Robert B. Hammond[a], Dimo Kashchiev[b], Kevin J. Roberts[a*], Ken Lewtas[c], Iain More[c]

[a] Institute of Particle Science and Engineering and Institute of Process Research and Development, School of Process, Environment and Materials Engineering, University of Leeds, Leeds, LS2 9JT, UK

[b] Institute of Physical Chemistry, Bulgarian Academy of Sciences, ul. Acad. G. Bonchev 11, Sofia 1113, Bulgaria

[c] Infineum UK Ltd, Milton Hill Business and Technology Centre, Abingdon, OX13 6BB, UK

Keywords: Solution Crystallisation, Polythermal and Isothermal Methods, Critical Undercooling, Relative Critical Undercooling, Nucleation, Instantaneous Nucleation, Progressive Nucleation, Biodiesel Fuels, Fatty Acid Methyl esters.

*Corresponding author

Submitted to the CrystEngComm, revised supplementary material 01th September 2013

ABSTRACT

Additional and more detailed materials are provided as a supplement to the paper with the above title. It includes:

1. Description of the Kashchiev-Borissova-Hammond-Roberts ($KBHR$) approach [1, 2] used for the analyses of solution crystallisation kinetics.
2. Sensitivity analysis of the experimental methodology for the collection of sufficient and reliable polythermal data.
3. Derivation of an expression allowing determination of a system nucleation mechanism from previous Nyvlt-type data analysis.

The reference numbering in the supplementary material coincides with that in the paper.

1. Detailed derivation of equations (10) and (21) in the paper from the Kolmogorov-Johnson-Mehl-Avrami ($KJMA$) expression

A detailed derivation of basic equations obtained within the framework of the Kashchiev-Borissova-Hammond-Roberts $KBHR$ approach [1, 2] is presented below. Using the classical nucleation theory and the $KJMA$ equation, expressions for the dependence of the critical undercooling on the cooling rate are derived for the cases of progressive nucleation (PN) and instantaneous nucleation (IN).

In solution crystallisation, the phase transformation kinetics can be described by the $KJMA$ equation [11]. The central idea of this equation is to focus on the increment in the fraction α of crystallised volume and to relate this increment to the current actual value of . The fraction of crystallised volume is defined as

$$\alpha = \frac{V_c}{V} \tag{1}$$

where V_c is the total crystallised volume and V the solution volume.

Obtaining the dependence of αon time t from the $KJMA$ equation can be a complicated mathematical problem, especially when the solution supersaturation and/or the crystal nucleation and/or growth rates vary with time. The $KJMA$ theory assumes that crystallisation occurs by nucleation of material points at a rate $J(t)$ which then only grow irreversibly in radial direction with growth rate $G(t)$ [11]. Under this assumption α can be easily expressed in terms of $J(t)$ and $G(t)$at the early stage of crystallisation when there are no contacts between the growing crystallites. The resulting $KJMA$ formula reveals how α is controlled by two

basic kinetic parameters of the process of crystallisation, the crystallite nucleation and growth rates [1, 2, 11].

1.1 Progressive nucleation

In the case of PN, the $KJMA$ formula can be represented as [1, 11]

$$\alpha(t) = k_v \int_0^t J(t') \left[\int_0^{t-t'} G(t'')dt'' \right]^d dt' \quad for\ \alpha < 0.1 \tag{2}$$

where t' and t'' are time integration variables, $d = 1,2,3$ is the dimensionality of crystallite growth (e.g., 3 for spheres or cubes, 2 for disks or plates, 1 for needles), and k_v (m^{3-d}) is the crystallite growth shape factor, e.g. $\frac{4\pi}{3}$ for spheres, 8 for cubes, πH_0 for disks, $4H_0$ for square plates, $2A_0$ for needles (H_0 is the fixed disk or plate thickness, A_0 is the fixed needle cross-sectional area).

When steady cooling of the solution starts at $t = 0$ from the equilibrium temperature T_e, the relative undercooling u is defined as [1]

$$u = \frac{\Delta T}{T_e} = \frac{T - T_e}{T_e} \tag{3}$$

where T is the solution temperature, and ΔT is the undercooling.

From the classical theory of three dimensional $(3D)$ nucleation, the rate of crystallite nucleation can be expressed in terms of the relative undercooling as [1]

$$J(t) = K_J e^{\frac{-b}{(1-u)u^2}} \tag{4}$$

where K_J is the nucleation rate constant and the dimensionless thermodynamic parameter b is given by

$$b = \frac{k_n v_o^2 \gamma_{eff}{}^3}{kT_e\lambda^2} \tag{5}$$

Here k_n is the nucleus numerical shape factor e.g. $(16\pi/3$ for spherical nuclei and 32 for cubic nuclei), v_o is the volume occupied by a solute molecule in the crystal, γ_{eff} is the effective interfacial tension of the crystal nucleus, λ is the molecular latent heat of crystallisation, and k is the Boltzmann constant

The radial crystallite growth rate $G(t)$ can also be expressed in terms of undercooling [1]:

$$G(t) = m\left(\frac{T_e}{q}\right)^{m-1} K_G^m \left[1 - e^{\frac{-au}{(1-u)}}\right]^{nm} u^{m-1} \tag{6}$$

Here q is the cooling rate, K_G is the crystal growth rate constant, and n and $m > 0$ are the crystallite growth exponents ($n = 1$ for growth mediated by diffusion or interface transfer of solute, $n = 2$ for growth controlled by the presence of screw dislocations in the crystallite, and m ranges between ½ and 1[1, 11, 18]). For instance [1, 11, 18], $m = 1/2$ for growth controlled

by undisturbed diffusion of solute, and $m = 1$ for growth by diffusion of solute through a stagnant layer around the crystal and for normal or spiral growth limited by transfer of solute across the crystal/solution interface. At $m = 1$ the crystallite growth rate is time-independent [1, 11, 18]. As to a, it is the dimensionless molecular latent heat of crystallisation and is given by

$$a = \frac{\lambda}{kT_e} \tag{7}$$

Inserting equation (4) and (6) in equation (2) and defining $t' = \left(\frac{T_e}{q}\right) x$ and $t'' = \left(\frac{T_e}{q}\right) z$ allows expressing α in terms of undercooling [1]:

$$\alpha(u) = C_{m,d} \int_0^u e^{\frac{-b}{(1-x)x^2}} \left(\int_0^{u-x} z^{m-1} \left[1 - e^{\frac{-az}{(1-z)}} \right]^{nm} dz \right)^d dx \tag{8}$$

where the dimensionless parameter $C_{m,d}$ is given by

$$C_{m,d} = k_v m^d K_J K_G^{md} \left(\frac{T_e}{q} \right)^{md+1} \tag{9}$$

The integrals in equation (8) can be performed analytically [17] if the analysis is restricted to small enough values of u satisfying the inequalities

$$u < 0.1, au < 1 \tag{10}$$

then

$$1-u \approx 1 \text{ and } 1-e^{\frac{-au}{(1-u)}} \approx au \tag{11}$$

and equation (8) becomes [1]

$$\alpha(u) = C_{m,d} a^{nmd} \int_0^u e^{\frac{-b}{x^2}} \left[\int_0^{u-x} z^{(n+1)m-1} dz \right]^d dx \tag{12}$$

which, after performing the inner integral, takes the form [1]

$$\alpha(u) = C_{m,d} \left[\frac{a^{nm}}{(n+1)m} \right]^d \int_0^u (u-x)^{(n+1)md} e^{\frac{-b}{x^2}} dx \tag{13}$$

It has been shown [1, 17] that the integration in equation (13) can be carried out analytically for any u value only when $(n+1)md = 0,1,2,3 \ldots$ .Then $\alpha(u)$ from equation (13) can be expressed exactly but n a rather complicated way by employing special mathematical functions [17]. However in the limit of sufficiently small u values satisfying the condition

$$u < \left(\frac{2b}{3}\right)^{1/2} \tag{14}$$

a series expansion of the special functions allows simplifying the exact complicated $\alpha(u)$ dependence and presenting it in the following approximate form [1]:

$$\alpha(u) = K_{m,d} \left(\frac{u^3}{2b}\right)^{(n+1)md+1} e^{\frac{-b}{u^2}} \tag{15}$$

Furthermore, it was found [1] that the accuracy of this $\alpha(u)$ dependence is higher when the exponential term in it is replaced by $e^{\frac{-b}{(1-u)u^2}}$. With this replacement, equation (15) yields the basic approximate $\alpha(u)$formula of the $KBHR$ theory [1]:

$$\alpha(u) = K_{m,d}\left(\frac{u^3}{2b}\right)^{(n+1)md+1} e^{\frac{-b}{(1-u)u^2}} \tag{16}$$

Here the dimensionless parameter $K_{m,d}$ is given by

$$K_{m,d} = \frac{\Gamma[(n+1)md+1]}{(n+1)^d} k_v a^{nmd} K_J K_G^{md} \left(\frac{T_e}{q}\right)^{md+1} \tag{17}$$

and Γ is the complete gamma function .

Upon replacing α by the number N of nucleated crystallites and setting $d = 0$, equation (16) leads to the approximate $N(u)$formula of the $KBHR$ theory [1]

$$N(u) = K_N\left(\frac{u^3}{2b}\right) e^{\left[\frac{-b}{(1-u)u^2}\right]} \tag{18}$$

where the factor K_N equals $K_{m,o}$ from equation (17) and, accordingly, is given by

$$K_N = \frac{VK_J T_e}{q} \tag{19}$$

Plotting the above $\alpha(u)$ and $N(u)$ dependence shows [1] that α and N are monotonically increasing functions of u, with a sharp rise at a certain u value that corresponds to the relative critical undercooling for crystallisation u_c defined as [1]

$$u_c = \frac{\Delta T_c}{T_e} \tag{20}$$

where

$$\Delta T_c = T_e - T_c \tag{21}$$

and T_c is the crystallisation temperature

For $u < u_c$ crystallites are so small and/or few that α and/or N cannot be detected, i.e. they are below the detection limit α_{det}, N_{det}, respectively . For $u > u_c$ the solution will contain sufficiently big and/or numerous crystallites so that α and/or N will be detected: $\alpha > \alpha_{det}$ and $N > N_{det}$. This means that u_c is the maximum relative undercooling that a solution can sustain without detectable crystallisation. In other words, u_c represents the solution metastability limit in terms of undercooling [1, 2]. This limit, however, depends on a number of parameters among which a prominent one is the solution cooling rate q. With the help of equations (16) and (18),the $u_c(q)$ dependence can be determined.

Expressing equation (18) it in terms of u_c gives

$$N(u_c) = N_{det} = \frac{VK_J T_e}{q}\left(\frac{{u_c}^3}{2b}\right) e^{\left[\frac{-b}{(1-u_c){u_c}^2}\right]} \tag{22}$$

Upon taking logarithms of both sides of equation (22) and rearranging, a model expression that relates the relative critical undercooling u_c with the cooling rate q is obtained [1]:

$$ln\, q = ln\, q_0 + a_1\, ln\, u_c - \frac{a_2}{(1-u_c){u_c}^2} \tag{23}$$

where the parameters q_0 , a_1 and a_2 are defined by

$$a_1 = 3 \tag{24}$$

$$a_2 = b \tag{25}$$

$$q_0 = \frac{VK_J T_e}{N_{det}\, 2b} \tag{26}$$

Similarly when equation (23) is derived by means of α from equation (16), the parameters q_0, a_1 and a_2 are defined by [1]

$$a_1 = 3 + \frac{3nmd}{md+1} \tag{27}$$

$$a_2 = \frac{b}{md+1} \tag{28}$$

$$q_0 = T_e \left\{ \frac{\Gamma[(n+1)md+1] K_v a^{nmd} K_J K_G^{md}}{(n+1)^d \, (2b)^{(n+1)md+1} \alpha_{det}} \right\}^{\frac{1}{(md+1)}} \tag{29}$$

The parameters $\ln q_0$, a_1 and a_2 have a clear physical meaning: a_1 is related solely with the crystallites growth law as its values is determined by the growth dimensionality d and exponents $n \; and m$, a_2 is a fraction of or is equal to the thermodynamic nucleation parameter b and q_0 is controlled by parameters of both the nucleation and the growth of the crystallites.

It is important to bring attention to the fact that although equation (16) is only an approximation to equation (8), applicable for u values restricted by inequalities (10) and (14), it predicts u_c values quite close to those resulting from equation (8). As visualised in Fig. 1 presented below [1] the error in u_c determined from the approximate equation (16) for $\alpha(u)$ can be estimated by comparing the numerically obtained u_c from equation (8) and the calculated approximate u_c from equation (16) or, equivalently, from equation (23). From Fig. 1[1] we read that for $n = 1$ and 2, while the exact u_c values equal 0.084 and 0.094, the approximate u_c values equal 0.083 and 0.091, which corresponds to errors of 2% and 3% respectively. Thus, inequalities (10) and (14) are appropriate for ensuring sufficient accuracy of the u_c values from the approximate equation (23). Fig. 2 [1] illustrates the good accuracy of this equation in a range of q values.

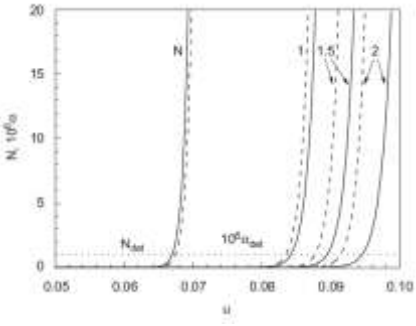

Fig. 1 Dependence of total crystalline number N and volume fraction α on relative undercooling at a fixed cooling rate: solid lines numerically from eq. (8), dashed lines the approximate eq. (16) and (18). 1, 1.5 and 2 refer to the volume fraction at n =1, 1.5 and 2 respectively. "Reproduced by consent of the Journal of Crystal growth from D. Kashchiev, A. Borissova, R.B. Hammond, K.J. Roberts, Effect of cooling rate on the critical undercooling for crystallization, Journal of Crystal Growth, 312 (2010) 698-704".

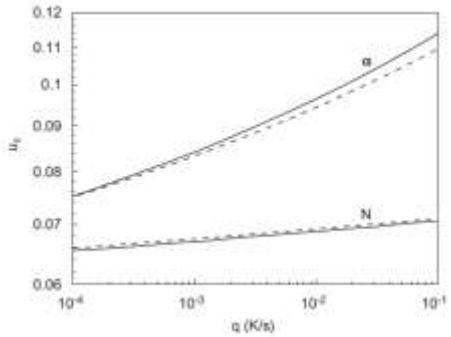

Fig. 2 $log - log$ dependence of relative critical undercooling on cooling rate: solid lines –numerically from eq. (8) and, dashed lines the approximate eq.(23). "Reproduced by consent of the Journal of Crystal growth from D. Kashchiev, A. Borissova, R.B. Hammond, K.J. Roberts, Effect of cooling rate on the critical undercooling for crystallization, Journal of Crystal Growth, 312 (2010) 698-704".

1.2 Instantaneous nucleation

In the case of IN, a similar derivation was done [2] but by taking into account that now all crystal nuclei with a concentration C_o appear at once at the moment t_o and after that they only grow. An example of IN is heterogeneous nucleation (HEN) on strongly nucleation-active sites. These sites are not active during the period from $t = 0$ to $t = t_o$, because then the undercooling is not sufficient for HEN to take place on them. At $t = t_o$ all sites are suddenly occupied by the nucleated crystallites so that for $t > t_o$ further HEN on them is impossible despite that the solution is being further cooled down. Thus, quite often C_o can be merely equal to the concentration of nucleation-active sites in the system.

As in the IN case the $\alpha(u)$ dependence is controlled solely by the crystallite growth rate, it can be expressed as [2]

$$\alpha(t) = k_v C_o \left[\int_{t_0}^{t} G(t')\, dt'\right]^d \tag{30}$$

Using equation (6) and setting $t' = \frac{T_e}{q}x$, an expression for α in terms of u can be found [2]

$$\alpha(u) = C_{m,d}\left(\int_{u_0}^{u} x^{m-1}\left[1 - e^{\frac{-ax}{(1-x)}}\right]^{nm} dx\right)^d \tag{31}$$

where the dimensionless parameter $C_{m,d}$ is given by

$$C_{m,d} = k_v m^d C_o \left(\frac{K_G T_e}{q}\right)^{md} \tag{32}$$

For small enough undercooling satisfying inequalities (10), the approximations (11) can be used to simplify and perform the integral in equation (31), the result being [2]

$$\alpha\,(u) = K_{m,d}\left[u^{(n+1)m} - u_o^{(n+1)m}\right]^d \tag{33}$$

In this expression u_o is the relative undercooling at the time t_o and is given by

$$u_o = \frac{\Delta T_o}{T_e} = \frac{q t_0}{T_e} \tag{34}$$

Here ΔT_o is defined by

$$\Delta T_0 = T_e - T_0 \tag{35}$$

where T_o is the solution temperature at the time t_o. As to the parameter $K_{m,d}$ in equation (33), it is given by

$$K_{m,d} = \frac{k_v C_o \left(\frac{a^n K_G T_e}{q}\right)^{md}}{(n+1)^d} \tag{36}$$

Equation (33) shows that, similar to the PN case, in IN-mediated crystallisation α is a monotonically increasing function of u ,with a sharp rise at a certain value that corresponds to the relative critical undercooling u_c (see Fig. 1 of Ref. [2]).

Upon using$\alpha(u_c) = \alpha_{det}$, taking logarithms of both sides of equation (33) and rearranging, an expression can be obtained for the dependence of the relative critical undercooling on the cooling rate [2]:

$$\ln q = \ln q_0 + \left(\frac{1}{m}\right) \ln\left[u_c^{(n+1)m} - u_0^{(n+1)m}\right] \tag{37}$$

In this expression $u_0 \geq 0$, $u_c > u_o$,and the parameter q_0 is given by

$$q_o = \left[\frac{k_v C_o}{(n+1)^d \alpha_{det}}\right]^{\frac{1}{md}} a^n K_G T_e \tag{38}$$

If the undercooling at which all nuclei spontaneously appear is small enough for the inequality

$$u_o^{(n+1)m} \ll u_c^{(n+1)m} \tag{39}$$

to be satisfied, equation (37) takes the simple form

$$\ln q = \ln q_o + (n+1) \ln u_c \tag{40}$$

It should be noted that comparison of equation (40) with the equation

$$ln\, q = ln\, q_0 + \left(3 + \frac{3nmd}{md+1}\right) ln\, u_c - \frac{a_2}{(1-u_c)u_c^2} \tag{41}$$

representing equation (23) for PN reveals how different the $u_c(q)$ function can be, depending on the mechanism by which the crystallite nucleation takes place. Whereas in the case of PN, this function contains parameters characterising both the nucleation and the growth of the crystallites, in the IN case the parameters in it are only related to the crystallite growth.

1.3 The crystallite growth shape factors

The crystallite growth shape factor k_v refers to the factor that relates the volume (V_n) and the effective radius (R) of an individual crystallite: $V_n = k_v(R)^d$ [11].

From this definition, the shape factor k_v is derived below for one-dimensional growth of needles with constant cross-sectional area A_0, for two-dimensional growth of disks or square prisms with constant thickness H_0 and for $(3D)$ growth of spheres or cubes [11].

Sphere, $R = R$ where R is the sphere radius:

$$V_{Sph} = \frac{4}{3}\pi R^3 = k_v R^3$$
$$k_v = \frac{4}{3}\pi$$

Cube, $R = \frac{L}{2}$ where L is the cube side length:

$$V_{cube} = L^3 = k_v R^3$$
$$(2R)^3 = k_v R^3$$
$$k_v = 8$$

Needle, $R = \frac{h}{2}$ where h is the needle height:

$$V_{need} = A_0 * h = k_v R^1$$
$$A_0 2R = k_v R$$
$$k_v = 2A_0$$

Disk, $R = R$ where R is the disk radius:

$$V_{disk} = A_{circumference} * H_0 = k_v R^2$$
$$\pi R^2 H_0 = k_v R^2$$
$$k_v = \pi H_0$$

Square plate, $R = \frac{L}{2}$ where L is the plate side length:

$$V_{Sq\ plate} = A_{square} * H_0 = k_v R^2$$
$$L^2 H_0 = k_v R^2$$
$$(2R)^2 H_0 = k_v R^2$$
$$4R^2 H_0 = k_v R^2$$

2. Sensitivity analysis of the experimental methodology to collect reliable polythermal experimental data for the application of the $KBHR$ approach

A polythermal methodology to experimentally collect a large enough set of crystallisation temperatures T_c was presented in the paper. Due to the stochastic nature of nucleation, the use of eight different cooling rates q at each solution concentration and ten temperature cycles at each cooling rate was suggested, the latter with the aim of reducing the standard deviation SD of the crystallisation temperatures T_c. However, the collection of all these data was not an easy task, as it required running 320 temperature cycles, each of which can last an average of three hours. Thus a sensitivity analysis for the applied experimental methodology was carried out. Three additional scenarios were used with the aim of assessing the influence that reducing the number of cooling rates and/or temperature cycles will have on the parameters calculated obtained by applying the $KBHR$ approach. The results are presented in Table 1 below.

In all cases the slopes of the best linear fit to the data are higher than three, still confirming that methyl stearate crystallises from kerosene by the PN mechanism. However the values of the slopes obtained from the original methodology (fourth scenario) can be up to 40% higher than those of the first scenario as in the case of 250 g/l solution concentration.

The higher correlation coefficients R^2 in all cases are obtained for the second scenario, in which the number of cooling rates was reduced by 50% in comparison to the original methodology (fourth scenario). On the other hand, for three of the concentrations analysed, the lowest correlation coefficients R^2 were obtained for those scenarios in which the number of crystallisation temperatures collected at each cooling rate was reduced from ten to three.

Table 1. Slopes of the best linear fit of the experimental data points plotted in $ln\, q$ vs $ln\, u_c$ coordinates and corresponding correlation coefficients: values of the three free parameters a_1, a_2 and $ln\, q_o$ obtained from the data fitting in $ln\, q$ vs u_c coordinates according to equation (23) and corresponding correlation coefficients. All values provided at four different concentrations 200, 250, 300 and 350 g/l and four different experimental methodologies scenarios.

4 cooling rates 3 temperature cycles at each cooling rate

Concentration (g/l)	Slope best fit data straight line of $\ln u_c \ Vs \ln q$	R^2linear fitting	a_1	$a_2 = b$	$\ln q_0$	$q_0\left(\frac{K}{s}\right)$	$\gamma_{eff}\left(\frac{mJ}{m^2}\right)$	$R^2 fitting\ equation\ (23)$
200	4.49±1.28	0.86	3	0.000365±3.016*10^{-4}	8.80±0.83	6634.51	1.43	0.86
250	3.45±0.82	0.90	3	0.000091±1.472*10^{-4}	8.49±0.57	4880.47	0.90	0.90
300	3.77±0.36	0.98	3	0.000157±3.713*10^{-5}	8.62±0.14	5515.71	1.08	0.99
350	3.91±0.95	0.89	3	0.000259±1.740*10^{-4}	8.83±0.57	6828.34	1.28	0.93

4 cooling rates 5 temperature cycles at each cooling rate

Concentration (g/l)	Slope best fit data straight line of $\ln u_c \ Vs \ln q$	R^2linear fitting	a_1	$a_2 = b$	$\ln q_0$	$q_0\left(\frac{K}{s}\right)$	$\gamma_{eff}\left(\frac{mJ}{m^2}\right)$	$R^2 fitting\ equation\ (23)$
200	4.92±0.81	0.95	3	0.000521±1.457*10^{-4}	8.98±0.37	7966.99	1.61	0.97
250	3.65±0.66	0.94	3	0.000132±1.091*10^{-4}	8.64±0.42	5639.20	1.02	0.95
300	4.22±0.36	0.99	3	0.000262±2.942*10^{-5}	8.70±0.093	5998.64	1.28	0.99
350	3.93±0.66	0.95	3	0.000239±1.029*10^{-4}	8.67±0.33	5847.78	1.25	0.97

8 cooling rates 3 temperature cycles at each cooling rate

Concentration (g/l)	Slope best fit data straight line of $\ln u_c \ Vs \ln q$	R^2linear fitting	a_1	$a_2 = b$	$\ln q_0$	$q_0\left(\frac{K}{s}\right)$	$\gamma_{eff}\left(\frac{mJ}{m^2}\right)$	$R^2 fitting\ equation\ (23)$
200	4.94±0.66	0.90	3	0.000531±1.802*10^{-4}	8.92±0.33	7488.15	1.62	0.90
250	3.92±0.52	0.91	3	0.000212±1.160*10^{-4}	8.55±0.27	5153.05	1.20	0.91
300	4.53±0.33	0.97	3	0.000410±7.279*10^{-5}	8.65±0.14	5719.92	1.49	0.98
350	4.93±0.57	0.93	3	0.000649±1.421*10^{-4}	8.90±0.24	7337.73	1.74	0.95

8 cooling rates 10 temperature cycles at each cooling rate

Concentration (g/l)	Slope best fit data straight line of $\ln u_c \ Vs \ln q$	R^2linear fitting	a_1	$a_2 = b$	$\ln q_0$	$q_0\left(\frac{K}{s}\right)$	$\gamma_{eff}\left(\frac{mJ}{m^2}\right)$	$R^2 fitting\ equation\ (23)$
200	5.17±0.57	0.93	3	0.000653±1.478*10^{-4}	8.97±0.26	7834.01	1.74	0.94
250	4.82±0.59	0.92	3	0.000543±1.471*10^{-4}	8.81±0.26	6673.54	1.64	0.93
300	5.05±0.47	0.95	3	0.000629±1.132*10^{-4}	8.83±0.19	6811.22	1.72	0.97
350	5.06±0.51	0.94	3	0.000698±1.258*10^{-4}	8.82±0.20	6761.14	1.79	0.96

As to the errors in the parameters, in the case of the linear fitting, the lowest errors in the slopes are obtained for those scenarios where eight cooling rates were used (third and fourth scenario). In the case of the fitting according to equation (23), for the parameter $\ln q_0$ in general, the lowest errors are reported again for the third and fourth scenarios, while for the parameter a_2, the lowest errors are for the second and fourth scenarios. It can be inferred

therefore that the number of cooling rates has less influence in improving the fitting of the data by either of the two models than the number of repetitions for crystallisation temperatures at each cooling rate. On the other hand, the use of a greater number of cooling rates seems to lead to lower errors in the parameters of the models.

In general, the best results in terms of data fitting and parameters errors were obtained for the second and fourth scenarios. In the former case, however, the effort in the collection of experimental data would be significantly reduced. It is also observed that the values of effective interfacial tensions γ_{eff} increase with increasing the number of cooling rates and the number of collected crystallisation temperatures at each cooling rate. These values in the fourth scenario can be between 8% to 60% greater than those in the second scenario. However, this difference only represents an increase of up to 0.6 $\left(\frac{mJ}{m^2}\right)$ in the values of the interfacial tension. Thus, the second methodology is recommended.

3. Analysis of experimental data using the Nyvlt approach and derivation of a correlation equation whereby the nucleation mechanism can be determined from previous Nyvlt-type data analysis

As already mentioned, Nyvlt [6] developed an original approach for the interpretation of $MSZW$ data obtained by the polythermal method. The approach is based on the well-known semi-empirical power law [6, 7]

$$J = k_j(\Delta \mathrm{C}_{max})^{m_0} \tag{42}$$

where k_j is an empirical parameter , m_0 is the order of nucleation, $\Delta C_{max} = C_{max} - C_e$ is the maximum concentration difference, C_{max} is the solution concentration at the metastability limit, and C_e is the solution equilibrium concentration or solubility.

Nyvlt suggested that a plot of the cooling rate q vs the critical undercooling ΔT_c in *ln-ln* coordinates will deliver the value of the nucleation order m_0 according to

$$\log q = (m_0 - 1)\log\frac{dC_e}{dT} + \ln k_j + m_o \ln \Delta T_c \tag{43}$$

Here ΔC_{max} and ΔT_c are related by

$$\Delta C_{max} = \frac{dC_e}{dT}\Delta T_c \tag{44}$$

and ΔT_c is defined by

$$\Delta T_c = T_{diss} - T_c \quad (45)$$

where T_{diss} is the dissolution temperature and T_c is the crystallisation temperature.

Using Nyvlt approach,ΔT_c values were calculated from the experimental data as the difference between the average dissolution and crystallisation temperatures at each cooling rate (see Table 2 below).

Table 2. Average dissolution and crystallisation temperatures as a function of cooling rate for methyl stearate in kerosene at 200, 250, 300 and 350 g/l. Corresponding critical undercooling calculated as the difference between dissolution and crystallisation temperatures.

q (°C /min)	T_c (°C)	T_{diss} (°C)	ΔT_c (°C)
200 g/l			
0.25	12.56	17.69	5.13
1	11.99	18.66	6.67
3.2	10.26	21.92	11.66
5	8.77	24.07	15.30
7	8.10	27.29	19.20
9	7.68	30.16	22.48
11	8.53	30.85	22.32
13	8.09	33.46	25.38
250 g/l			
0.25	14.88	19.59	4.71
1	14.16	20.81	6.65
3.2	12.15	24.85	12.71
5	10.82	28.49	17.67
7	10.27	31.88	21.61
9	9.09	34.12	25.02
11	10.49	36.30	25.81
13	10.54	38.78	28.24
300 g/l			
0.25	16.54	21.03	4.49
1	15.29	22.46	7.17
3.2	13.96	26.87	12.91
5	12.95	29.88	16.93
7	11.53	33.68	22.14
9	10.82	35.88	25.06
11	11.66	37.30	25.65
13	11.80	40.03	28.23
350 g/l			
0.25	17.75	22.19	4.43
1	16.85	23.71	6.86
3.2	15.12	28.29	13.17
5	14.33	31.44	17.11
7	13.31	35.36	22.06
9	11.69	37.52	25.84
11	12.86	38.96	26.11
13	12.91	40.12	27.21

At each concentration, the obtained values for ΔT_c were plotted as a function of the cooling rate q in $ln - ln$ coordinates and fitted by a straight line. According to the Nyvlt-type

equation (43), the slope of the line delivers the nucleation order m_0. Fig. 1 below exemplifies the plot for methyl stearate in kerosene at 200 g/l.

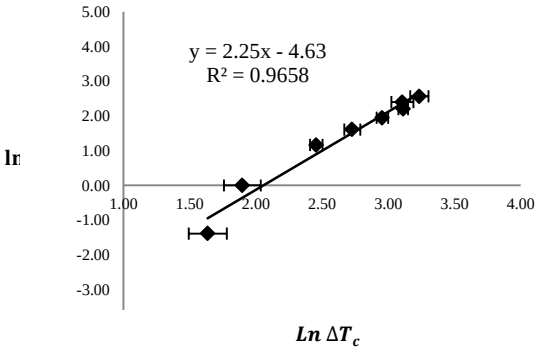

Fig. 1 Plot of experimental data collected by means of the polythermal methodology in $ln\ q$ vs $ln\ \Delta T_c$ coordinates for methyl stearate in kerosene at a concentration of 200 g solute per litre of solvent. $\Delta T_c = T_{diss} - T_c$

The obtained nucleation order, correlation coefficient, parameter standard deviations and covariance at each concentration are given in Table 3 below.

Table 3. Nucleation order as a function of concentration and correlation coefficient of experimental data plotted in $ln\ q$ vs $ln\ \Delta T_c$ coordinates as well as standard deviation and covariance of the corresponding parameters of the linear fitting.

$Concentration\ (g/l)$	$slope\ /Nucleation\ order\ (m_0)$	R^2	Slope Standard Deviation (SD)	Intercept Standard Deviation (SD)	Covariance Slope/Intercept
200	2.2±0.17287	0.97	0.63	1.71	-1.06
250	2.0±0.12701	0.98	0.56	1.57	-0.86
300	2.0±0.11204	0.99	0.56	1.58	-0.87
350	2.0±0.10292	0.98	0.56	1.55	-0.84

The slopes of the lines in all cases show that the nucleation order m_0 in equation (42) approximates two. As expected, the slopes of the best linear fit of the collected data using the Nyvlt approach [6, 7] are lower than those obtained from the best linear fit using the $KBHR$ approach. This is so because in the case of $KBHR$ approach, as derived analytically, the critical undercooling ΔT_c is defined as the difference between the solution equilibrium temperature T_e and the corresponding crystallisation temperature T_c .

On the other hand in the case, in the case of the Nyvlt approach, as derived from an empirical expression, the critical undercooling ΔT_c is defined as the difference between the dissolution temperatures T_{diss} and the corresponding crystallisation temperature T_c. The equilibrium temperatures are always lower than the dissolution ones, because they are obtained by extrapolating to zero cooling rate the straight lines that fit best the $T_{diss}(q)$ data and because T_{diss} increases with q.

Nonetheless, it might be possible to analytically establish a relationship between the slopes obtained by applying the Nyvlt approach and those obtained by applying the $KBHR$ approach. In the case of the former approach, data are plotted on $Ln\ q\ vs\ \ ln\,\Delta T_c$ coordinates with $\Delta T_c = T_{diss} - T_c$. Then an approximation of the slope (s_1) of the best linear fit to the data could be obtained by choosing two experimental data pairs $(T_{c1}, T_{diss1})$and (T_{c2}, T_{diss2}) of the dissolution and crystallisation temperatures and using them in the following expression

$$s_1 = \frac{ln\,q_2 - ln\,q_1}{ln\,\Delta T_{c2} - ln\,\Delta T_{c1}} = \frac{ln\,q_2 - ln\,q_1}{ln(T_{diss2} - T_{c2}) - ln\,(T_{diss1} - T_{c1})} \tag{46}$$

This approximation could only holds if the bets linear fit to the experimental data according to the Nyvlt approach has a reasonable correlation coefficient R^2.

The same principle can be applied to obtain an approximation of the slope (s_2) of the best linear fit to data plotted in $ln\,q\ vs.ln\,u_c$ coordinates according to $KBHR$ approach with $u_c = \frac{\Delta T_c}{T_e} = \frac{T_e - T_c}{T_e}$, thus

$$s_2 = \frac{ln\, q_2 - ln\, q_1}{ln\, u_{c2} - ln\, u_{c1}} = \frac{ln\, q_2 - ln\, q_1}{ln\left(\frac{T_e - T_{c2}}{T_e}\right) - ln\left(\frac{T_e - T_{c1}}{T_e}\right)} = \frac{ln\, q_2 - ln\, q_1}{ln(T_e - T_{c2}) - ln(T_e - T_{c1})} \quad (47)$$

As T_e is greater than any of the experimentally collected dissolution temperatures T_{diss} by a known value Δ_T, equation (47) can be expressed as

$$s_2 = \frac{ln\, q_2 - ln\, q_1}{ln(T_{diss2} - T_{c2} - \Delta_{T2}) - ln(T_{diss1} - T_{c1} - \Delta_{T1})} \quad (48)$$

The numerators of expressions (46) and (48) are equal, therefore

$$s_1[ln(T_{diss2} - T_{c2}) - ln\,(T_{diss1} - T_{c1})] = s_2[ln(T_{diss2} - T_{c2} - \Delta_{T2}) - ln(T_{diss1} - T_{c1} - \Delta_{T1})]$$

From this equality the $KBHR$ slope s_2 could be estimated from the Nyvlt slope s_1 by means of the formula

$$s_2 = \frac{s_1[ln(T_{diss2} - T_{c2}) - ln\,(T_{diss1} - T_{c1})]}{[ln(T_{diss2} - T_{c2} - \Delta_{T2}) - ln(T_{diss1} - T_{c1} - \Delta_{T1})]} \quad (49)$$

Again the accuracy with which s_2 can be predicted from s_1 by using equation (49) will greatly depend on the expected correlation coefficient R^2 of the best linear fit to experimental data points by applying both the $KBHR$ and the Nyvlt approaches. In general, from analysis of previously obtained experimental data, the values of s_2 were observed to be between 1.5 to 2.5 higher than those of s_1. Using these approximations for the case of methyl stearate crystallising from kerosene, the $KBHR$ slope s_2 will be in the range from 3-5,

because $m_0 = s_1 = 2$. This indicates that methyl stearate crystallises from kerosene by the PN mechanism, which is in agreement with the polythermal analysis presented in the paper.